

# Low-Cost Hydrogen Sensor in the ppm Range with Purely Optical Readout

Ediz Herkert, Florian Sterl,\* Nikolai Strohfeldt, Ramon Walter, and Harald Giessen

Cite This: *ACS Sens.* 2020, 5, 978–983

Read Online

ACCESS |



Metrics &amp; More



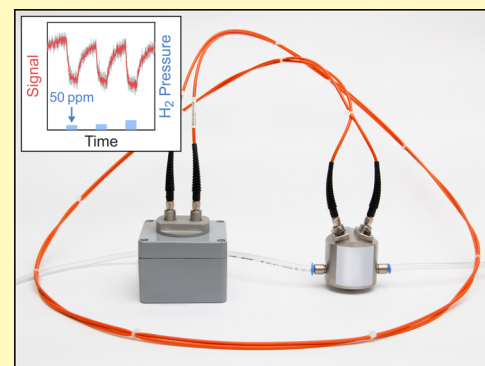
Article Recommendations



Supporting Information

**ABSTRACT:** Due to the changing global climate, the role of renewable energy sources is of increasing importance. Hydrogen can play an important role as an energy carrier in the transition from fossil fuels. However, to ensure safe operations, a highly reliable and sensitive hydrogen sensor is required for leakage detection. We present a sensor design with purely optical readout that reliably operates between 50 and 100,000 ppm. The building block of the sensor is a reactive sample that consists of a layered structure with palladium nanodisks as the top layer and changes its optical properties depending on the external hydrogen partial pressure. We use a fiber-coupled setup consisting of an LED, a sensor body containing the reactive sample, and a photodiode to probe and read out the reflectance of the sample. This allows separation of the explosive detection area from the operating electronics and thus comes with an inherent protection against hydrogen ignition by electronic malfunctions. Our results prove that this sensor design provides a large detection range, fast response times, and enhanced robustness against aging compared to conventional thin-film technologies. Especially, the simplicity, feasibility, and scalability of the presented approach yield a holistic approach for industrial hydrogen monitoring.

**KEYWORDS:** hydrogen, hydrogen detection, plasmonics, optical sensing, large-area nanofabrication, palladium, thermodynamics



Sustainable solutions for energy generation and storage are inevitable to reduce the effects of climate change. Hydrogen plays a key role in the transition to a climate-neutral energy grid due to its efficient and pollution-free applicability as chemical energy storage. Its capabilities as power-to-gas energy storage for renewable energy sources and as a fuel for sustainable mobility concepts have been examined extensively in recent years.<sup>1,2</sup> However, due to the flammability of hydrogen, the increasing amount of commercially available hydrogen storages requires economically feasible but highly reliable hydrogen monitoring systems. Besides that, robust and sensitive hydrogen sensors are also needed for other applications like the surveillance of incipient transformer failure.<sup>3,4</sup> Currently, there are various electronically operated hydrogen sensors that are based on catalytic combustion or thermal and electrical conductivity measurements. Unfortunately, the electronic readout of the sensing element is often disadvantageous if inherent safety, compactness, and inline operations at harsh conditions are required. Optically driven sensor designs can overcome these challenges since they allow separation of the contactless optical readout from the electronic post-processing and are thus also inherently protected against unintended hydrogen ignition by electronic malfunctions. The recent advances in nanofabrication and plasmonics gave rise to a variety of novel applications.<sup>5–10</sup> It particularly enabled a large number of approaches for purely optical and highly sensitive hydrogen sensors.<sup>11–20</sup> While most

of these approaches have provided novel materials and nanostructure compositions for the chemically active sample, they have not yet proven the feasible integrability into a compact and robust sensor design. For this reason, this publication aims to present a holistic and cost-efficient sensor concept that operates from 50 to 100,000 ppm ambient hydrogen and is consistently optimized for industrial requirements. While the presented sensor concept allows an easy integration of different reactive sample types, we utilize a low-cost and highly scalable multilayer structure with palladium nanodisks as the reference system.

The sensor consists of three major parts. A reactive sample is embedded in the sensor body that is situated in the sensing area. Spatially separated electronics power the light-emitting diode (LED) and the photodiode (PD). The LED (Roithner LED780-PD010-40D52) and PD (Osram SFH203P) are connected to the sensor body only with collimators (Thorlabs F220 SMA-B) and optical fibers (Thorlabs M37L02) so that all electronic parts can be safely operated far outside of the potentially explosive environment. Figure 1b demonstrates the

**Received:** November 22, 2019

**Accepted:** February 10, 2020

**Published:** February 10, 2020

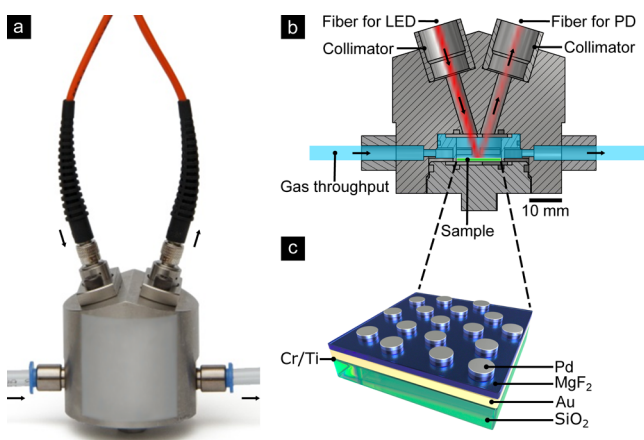


**Figure 1.** Design of the sensor body and reactive sample. (a) The body of the sensor is made of stainless steel. Two optical fibers on top of the sensor connect the reactive sample with the external LED and PD. The gas flow is ensured by the pipes on the sides of the sensor. (b) Light from an LED impinges on the surface of the reactive sample with an angle of  $17^\circ$ , and the reflected light is coupled into the PD fiber. The position of the sample in the sensor body assures laminar gas flow on the sample surface. (c) A layered structure on top of a glass substrate constitutes the reactive sample. The dielectric  $\text{MgF}_2$  layer separates the lower gold mirror and the top palladium nanodisks, which provides enhanced sensitivity to hydrogen exposure.

sensing principle, which is based on nearly monochromatic optical reflectance measurements. The light from the LED is coupled into the sensor body via a fiber and illuminates the reactive sample, which reflects the light toward the fiber-coupled PD. The reactive sample is designed such that the amount of reflected light critically depends on the hydrogen content in the vicinity of the sample, yielding a hydrogen concentration-dependent reflection signal. While the sample design is deduced from the plasmonic perfect absorber presented by Liu et al.,<sup>12</sup> the top layer consists of palladium nanostructures that are fabricated with the financially feasible and highly scalable colloidal etching lithography.<sup>21</sup> Palladium nanostructures have established themselves as reference hydrogen sensing materials due to their short response times and significant but reversible change of the optical properties upon hydrogen exposure at room temperature.<sup>11,13,18,20</sup>

The perfect absorber design provides robustness against fluctuations of the incidence angle and polarization with enhanced relative reflectance changes due to the strong absorbance in the absence of hydrogen.<sup>22,23</sup> Slightly higher reflectances are preferred in this study since recent work has suggested that this can be beneficial for the sensor sensitivity.<sup>24</sup> Nevertheless, the samples are designed such that the reflectance of the nanostructured samples is lowest in the absence of hydrogen and increases with the amount of ambient hydrogen. This enables to infer the hydrogen partial pressure from the reflected intensity using a suitable physical model that links the optical and thermodynamic quantities.<sup>25</sup> The computational modeling is primarily possible due to the well-examined thermodynamics of the interaction of hydrogen with palladium nanoparticles.<sup>26–31</sup>

To prevent the sensor signal from being disturbed by mechanical movements or misalignments, the sensor body has a thread-based architecture that provides tight fastening of the collimators and the fibers. The sample holder is specifically designed to prevent any sample movement. Besides these

mechanical measures, the disordered arrangement of the Pd nanostructures provides a highly angle-independent optical response due to the disorder-induced broadening of diffraction effects.<sup>23,24</sup> A detailed analysis of the positional ordering of the nanostructures can be found in the Supporting Information.

## EXPERIMENTAL RESULTS AND DISCUSSION

The chemically active sample consists of a silica substrate with a gold mirror as the bottom layer, a magnesium fluoride ( $\text{MgF}_2$ ) spacer layer, and the palladium nanodisks as the top layer. A thin chromium (Cr) or titanium (Ti) adhesion layer with a thickness of around 5 nm is used for better stability of the gold layer. The dimensions of the  $\text{MgF}_2$  spacer layer and the palladium nanostructures are decisive for the sensitivity and the optical properties of the sensor, while the thickness of the gold layer (120 nm) only needs to be clearly above the skin depth to avoid transmission. Here, 100 nm  $\text{MgF}_2$  and 20 nm Pd are deposited onto the substrate with electron beam vapor deposition. Colloidal etching lithography is carried out using polystyrene (PS) beads with a diameter of 220 nm and follows the methodology that is described by Walter et al.<sup>21</sup> Figure S6 indicates that using PS beads of this diameter yields palladium disks with a diameter of roughly 250 nm. The fabrication process enables tunable plasmonic resonances in the visible and near-infrared wavelength range, with macroscopic sample extents up to several centimeters. The resonance frequency and scattering characteristics of the sample can be easily tuned by changing the diameter of the PS beads and changing the spacer thickness. The former also provides a tuning method for the sample response time as it affects the surface-to-volume ratio of the palladium disks.

The data presented in this work is either acquired with the sensor unit in Figure 1 or with a bright-field microspectroscopy setup that provides the possibility to spectrally characterize the reactive samples and to modify the ambient temperature for isothermal measurements.

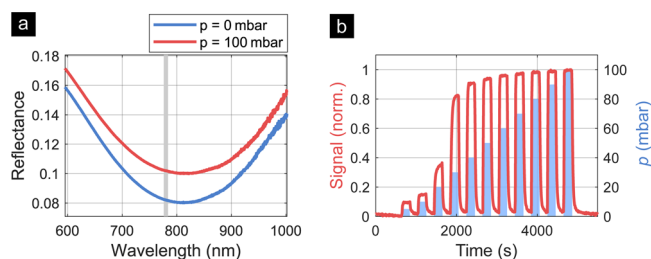


**Figure 2.** Sensing concept. The data is acquired using a bright-field microspectroscopy setup. (a) Changing the hydrogen partial pressure from 0 to 100 mbar changes the lineshape of the plasmonic resonance. This allows for either tracking the resonance wavelength or reading out the reflected intensity at a certain wavelength. Since the latter is more feasible for a compact and cost-efficient sensor design, the reflected intensity is read out at 780 nm in this case. (b) Tracking the normalized and baseline-corrected reflectance at 780 nm while varying the hydrogen partial pressure leads to a hydrogen concentration-dependent sensor response. A strong signal shift that originates from the phase transition of the palladium nanodisks can be observed at external hydrogen partial pressures above 20 mbar.

The microspectroscopy setup consists of a Princeton Instruments IsoPlane 160 grating monochromator with a Peltier-cooled Princeton Instruments PIXIS 256 CCD camera that is attached to a Nikon Eclipse LV100 upright microscope. In this setup, the reactive sample is placed in a custom-made gas flow cell that is temperature-controlled with a Peltier element and a Meerstetter Engineering TEC controller. The microspectroscopy setup is used to examine the optical and thermodynamic characteristics of the chemically active sample. We assume that this is a valid measure for assessing the sensor unit performance as the signal dynamics are mainly determined by the reactive sample and less by the measurement environment.

Comparing the data recorded with both setups (e.g., the phase transitions in Figures 3a and 5) indicates that this is a valid assumption.

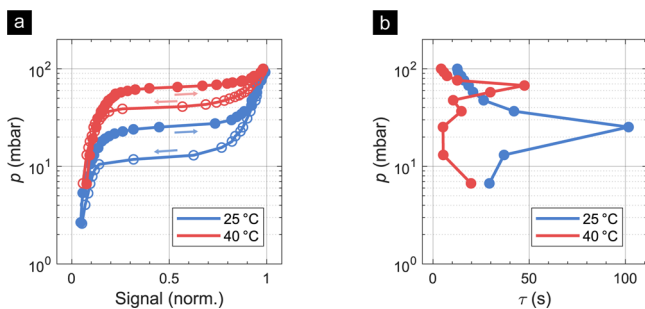


**Figure 3.** Temperature dependence and hysteresis of the saturation signal and signal rise time. The isothermal data was recorded at 25 and 40 °C with a microspectroscopy setup and evaluated at 600 nm. The signal in panel (a) is assumed to be linearly proportional to the hydrogen concentration in the palladium nanodisks. Filled/empty circles correspond to the absorption/desorption phase of the hydrogen into the palladium nanodisks. The decreased equilibrium signal at higher temperatures indicates that less hydrogen is incorporated in the palladium lattice. This effect shifts the palladium phase transition to higher external hydrogen partial pressures, which consequently extends the sensing range of the sensor unit. The 10–90% signal rise times  $\tau$  are shown in panel (b) in dependence of different external hydrogen partial pressures. The response times unveil that the diffusion is enhanced at higher temperatures and significantly slows down at the phase transition from  $\alpha$ - to  $\beta$ -phase palladium.

Independent of the optical measuring setup, the required  $H_2/N_2$  mixtures and flow rates are set with Coriolis mass flow controllers (Bronkhorst). The gas flows perpendicular to the sample surface to ensure a constant gas concentration at the sample site. Special care has been taken in the sensor design to ensure laminar gas flow within the sensor body. All measurements are conducted at a total ambient pressure of 1 atm so that the gas concentrations can be deduced from their partial pressures according to Dalton's law. The sensor performance is typically probed by stepwise increasing and decreasing the hydrogen concentration with intermediate nitrogen flushing steps to assess the sensor response and recovery times. This is only different for the acquisition of the pressure–composition isotherms in Figure 3a for which the hydrogen concentrations are gradually increased and decreased.

Figure 2 demonstrates the sensing principle using spectral data from the microspectroscopy setup. In the absence of hydrogen, a broad plasmonic resonance with low reflectance is observed. Exposing the sample to hydrogen causes changes in the spectrally resolved reflectance due to the hydrogenation of the palladium nanostructures. The idea behind the deployed measuring scheme is to record the reflectance of the sample at a single wavelength and thereby track the  $H_2$ -dependent change of the reflected intensity. These monochromatic reflectance measurements offer an easy to implement measuring scheme that can be adapted effortlessly to the needs of the specific application. However, this sensor concept requires wise selection of the readout wavelength to ensure optimal sensor performance. While it remains a good rule of thumb to choose the wavelength at the resonance flanks, the precise determination of the optimal wavelength is also dependent on the presence of noise. An effective methodology to determine a suitable readout wavelength is presented in Figure S3. This methodology could be included as part of the sensor calibration with regard to industrial applications. Figure 3 indicates that the signal depends highly nonlinearly on the applied hydrogen concentration. Additionally, hysteresis of the measured signal is observed so that the signal depends not only on the current hydrogen partial pressure but also on the previously applied partial pressures. The signal

nonlinearity and hysteresis are due to the phase transition from  $\alpha$ - to  $\beta$ -phase palladium upon hydrogen exposure above a critical hydrogen partial pressure.<sup>26,32</sup> The critical pressure depends not only on the ambient temperature but generally also on the dimensions of the palladium nanostructures. Furthermore, the phase transition also affects the diffusion coefficient,<sup>25</sup>

$$D_H = D_0 \exp\left(-\frac{\Delta E_a}{RT}\right) \frac{1}{2} \frac{\partial \ln p_{H_2}}{\partial \ln c_H} \quad (1)$$

which determines the diffusion rate of hydrogen atoms into the palladium lattice and thus the response time of the sensor. In this notation,  $D_0$  is a scaling factor,  $\Delta E_a$  is the activation energy,  $R$  is the ideal gas constant,  $T$  is the temperature,  $p_{H_2}$  is the external hydrogen partial pressure, and  $c_H$  is the H/Pd fraction within the palladium nanostructures. In plasmonics, it is commonly assumed that the signal changes linearly with  $c_H$ ,<sup>19,27,33–35</sup> which is why Figure 3a can be understood in terms of a pressure–composition isotherm though showing the pressure–signal dependency. The slopes of these pressure–composition isotherms allow estimation of the signal rise time by assuming correlation between the rise time and the diffusion coefficient in eq 1. Figure 3 demonstrates that this results in a very good qualitative agreement with the experimentally acquired 10–90% signal rise times for different temperatures. Higher temperatures are usually beneficial for the sensor performance since the nonlinear phase transition takes place at higher hydrogen partial pressures while the response times are significantly shortened. However, especially for compact inline measurements, there is often no possibility to influence the present conditions. For that reason, Teutsch et al. have shown that it is indeed possible to model the temperature-dependent, nonlinear, and hysteretic sensor response of the chemically active sample that is discussed here.<sup>25</sup> Furthermore, it has been shown recently that a substantially less complex sensor response is obtained by alloying the palladium with relatively high amounts of gold<sup>19,20,35,36</sup> or using tantalum (Ta)- and hafnium (Hf)-based samples at relatively high temperatures (90–120 °C).<sup>34,37</sup> Depending on the user requirements, this can be utilized to further simplify the usability and analysis of the sensing scheme presented in this work.

The previously discussed microspectroscopy measurements examined the critical processes within the reactive sample. However, to reliably evaluate the presented sensing scheme, it is essential to verify the performance of the reactive sample within our custom-made sensor unit. Figures 4 and 5 review the holistic sensor design for three requirements vital for most industrial gas sensing applications. These requirements involve the lower sensing limit, the signal stability, and aging effects that affect the dynamics and sensitivity of the sensor.

The arguably most relevant requirements for hydrogen sensors are the detection range and particularly the lower sensing limit. The pressure–composition isotherms in Figure 3 vividly demonstrate that the signal shifts are distinguishable up to approximately 100,000 ppm. This is sufficient for most sensing applications due to the lower explosion limit of hydrogen at about 40,000 ppm.<sup>38</sup> In contrast to that, the requirements for the lower sensing limit are highly dependent on the specific use case. While the monitoring of incipient transformer failure requires a reliable sensor performance around 500 ppm,<sup>3</sup> leakage detection in high-pressure electrolysis facilities might require the detection of even lower hydrogen levels. Nevertheless, common specifications of the lower sensing limit range 100–1000 ppm.<sup>39,40</sup> Exposing the sensor unit for 200 s to different  $H_2/N_2$  mixtures between 50 and 2000 ppm reveals that the lower sensing levels are covered very well by the sensor. Since the signal-to-noise ratio at 50 ppm hydrogen is just above 1, this is defined as the lower sensing limit of the presented sensor unit. The curved baseline in the low-concentration measurements originates from the incomplete desorption of hydrogen in the palladium nanodisks and can be avoided by using longer flushing cycles. The longer response time is likely due to the low probability that hydrogen molecules are adsorbed at the palladium surface at such low concentrations.

Remarkable signal stability is observed at low concentrations of 300–10,000 ppm and a gas exposure time of 600 s (Figure 4b). In this case, no nonlinear baseline is present because of the longer gas exposure time, which allows full dehydrogenation of the palladium nanostructures. This reconfirms that the nonlinear baseline in Figure 4a is indeed due to incomplete dehydrogenation. The signal rise and recovery times, as well as the signal shifts, remain almost constant during more than 4 h of permanent H<sub>2</sub>/N<sub>2</sub> exposure. The signal actually barely changes over more than 12 h, as depicted in the Supporting Information (Figure S2). This indicates that the presented sensor unit operates reliably under repeated hydrogen exposure. This short-term stability originates not least from the freedom of spatial expansion of the palladium nanostructures during the hydrogen incorporation. Because of that, nanostructures are more resistant against stresses and strains during hydrogenation compared to thin-film-based hydrogen sensors without adhesion layers.<sup>47</sup>

While palladium nanostructures are very robust against stress-induced damage, they are particularly susceptible to catalytic deactivation due to poisoning with carbon monoxide, nitrogen dioxide, and sulfur.<sup>20,42</sup> Figure 5 demonstrates how the sensor response is strongly affected by aging effects. Especially, the time constants are significantly lowered after storing the reactive sample for 4 months at standard conditions (approx.  $T = 20\text{ }^{\circ}\text{C}$  and  $p = 1\text{ atm}$ ). However, the performance of the sample can be partially restored by heating the reactive sample at  $160\text{ }^{\circ}\text{C}$  for 2 h. While this almost fully recovers the equilibrium signal, the signal rise and recovery times remain particularly worse at hydrogen partial pressures around the palladium phase transition. However, frequently heating the sample during automated maintenance intervals at optimized temperatures and heating durations is a promising approach to significantly lower the effects of poisoning. This heating procedure can safely be carried out in situ at the sensing site since the autoignition temperature of hydrogen in air is around  $500\text{ }^{\circ}\text{C}$ <sup>43</sup> and is thus significantly higher than the required maintenance temperatures. Currently, there are two major options that enable in situ heating of the reactive sample. First, it is possible to utilize the highly light absorbing reactive sample to introduce heat by adequately increasing the optical power of the light source. While this is certainly the most compact and viable option, it requires good control over the optical power and a relatively powerful light source. The second option to introduce heat into the sensor is by heating the mechanical sensor body with, for example, oil-based heat exchangers. Both options provide the possibility to heat the reactive sample without requiring electronics at the sensor site and therefore are particularly suitable for the presented sensor concept.

There are also various approaches to prevent the palladium poisoning instead of recovering the sample performance after the poisoning. Most of these approaches are based on chemically active diffusion barriers. Strohhfeldt et al.<sup>15</sup> have utilized a 3 nm thick platinum capping layer that significantly reduces aging of thin-film and nanostructured palladium-based hydrogen sensor designs. Similarly, Nugroho et al.<sup>20</sup> have suggested that a 35 nm PMMA coating can be utilized as a selective membrane that provides strongly improved protection against various trace gases and simultaneously reduces the sensor response time. Thus, by combining the protective layers with the heating procedure presented in this work, it is possible to obtain a very fast, sensitive, and financially feasible sensor design with highly enhanced long-term stability.

## CONCLUSIONS

In this work, we have presented a financially feasible sensor design that does not limit itself to the discussion of a novel chemically active sample design but also provides a holistic and industrially applicable sensor setup. Despite the simplicity of the nearly monochromatic reflectance measurements, a lower detection limit of only 50 ppm hydrogen and short 10–90% response times of a few tens of seconds were achieved. This remarkable performance was enabled by the nanostructured palladium disks that provide a high surface-to-volume fraction

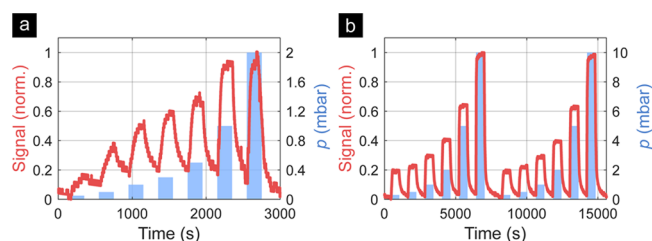


**Figure 4.** Lower sensing limit and signal stability. (a) Low hydrogen pressures down to 0.05 mbar (50 ppm, leftmost blue bar) can still be distinguished from the electronic noise at a readout wavelength of 780 nm. The nonlinear baseline is due to the incomplete dehydrogenation of the palladium that results from a short gas exposure time of only 200 s. (b) The signal remains stable during the full measurement period of more than 4 h. No nonlinear baseline is present anymore due to a longer gas exposure time of 600 s. This reinforces the finding that the observed baseline drifts mainly originate from incomplete dehydrogenation of the palladium nanodisks. In fact, the signal is very stable for almost 12 h as it is shown in Figure S2 of the Supporting Information. The reflected intensities are recorded using the custom sensor design and are linearly baseline-corrected and subsequently normalized.

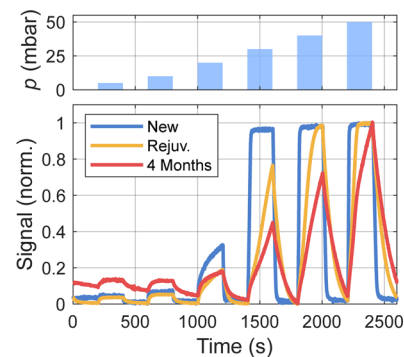


**Figure 5.** Aging of the reactive sample. Incorporation of sulfides, carbon monoxide, and other molecules in the lattice of the palladium nanodisks perturbs the diffusion dynamics in the plasmonic structure. This noticeably slows down the response time of the hydrogen sensor. However, heating the reactive samples for 2 h at  $160\text{ }^{\circ}\text{C}$  rejuvenates the sample and partially restores the sensor dynamics. The measurements are performed at 780 nm using the custom sensor design, and all reflected intensities are linearly baseline-corrected and normalized.

and the multilayered sensor design deduced from the idea of plasmonic perfect absorbers.<sup>12,22</sup> The careful selection of the readout wavelength plays a key role in optimizing the sensor performance (see Figure S3). It was shown that the highly nonlinear, hysteretic, and temperature-dependent sensor response originates from the thermodynamic nature of the palladium (de)hydrogenation that can be modeled with appropriate physical models.<sup>25</sup>

This is an important milestone toward the efficient determination of ambient hydrogen concentrations from the corresponding signal change of purely optical hydrogen sensor designs. Moreover, the presented sensor exhibits excellent short-term stability while being repeatedly exposed to low hydrogen contents over several hours. Strong degradation of the sensor performance is observed only after a few months due to poisoning with ambient trace gases. The initial performance was partially restored by a dedicated heating procedure of the reactive sample. An improved maintenance

scheme that promises to lower irreversible sample damage was proposed in this work. Complementing this in situ maintenance scheme with protective platinum, PMMA, or PMMA-PTFE tandem coatings is a very promising option to provide enhanced robustness of palladium-based reactive samples with long-term stability at harsh environmental conditions.<sup>15,20</sup> Furthermore, recent studies have indicated that good signal stability in synthetic air is provided by ternary PdAuCu systems.<sup>44</sup> The simple integrability of such samples into the presented sensor unit stresses the flexibility of the presented architecture and can yield one of the first purely optical and industrially applicable hydrogen sensors that meets most of the specifications<sup>39</sup> with hardly any need for further cost, compactness, and performance optimizations. Improved readout electronics and an ultrastable current source could possibly take our sensor into the single-digit ppm region. Nevertheless, we want to emphasize that not only the lower detection limit determines the suitability of a sensor for a certain industrial application. Since the precise requirements depend on the operational scenario, our sensor body architecture is designed to work with any reactive sample that changes the reflectivity upon hydrogen exposure. A comprehensive review on a large number of potentially suitable optical hydrogen sensors is provided by Zhang et al.<sup>45</sup>

## ■ ASSOCIATED CONTENT

### Supporting Information

The Supporting Information is available free of charge at <https://pubs.acs.org/doi/10.1021/acssensors.9b02314>.

Description of the baseline correction and normalization process; full data set of the measurement shown in Figure 4b; discussion of the influence of the readout wavelength; demonstration of the isothermal data acquisition process; multiple measurements with the sensor unit around the lower detection limit with specification of the 10–90% response times; SEM image and structure parameters of one of the reactive samples used for the data acquisition (PDF)

## ■ AUTHOR INFORMATION

### Corresponding Author

Florian Sterl – 4th Physics Institute and Research Center  
SCoPE, University of Stuttgart 70569 Stuttgart, Germany;  
orcid.org/0000-0002-1025-6777; Email: [f.sterl@pi4.uni-stuttgart.de](mailto:f.sterl@pi4.uni-stuttgart.de)

### Authors

Ediz Herkert – 4th Physics Institute and Research Center  
SCoPE, University of Stuttgart 70569 Stuttgart, Germany;  
orcid.org/0000-0003-3040-8077

Nikolai Strohfeldt – 4th Physics Institute and Research Center  
SCoPE, University of Stuttgart 70569 Stuttgart, Germany

Ramon Walter – 4th Physics Institute and Research Center  
SCoPE, University of Stuttgart 70569 Stuttgart, Germany

Harald Giessen – 4th Physics Institute and Research Center  
SCoPE, University of Stuttgart 70569 Stuttgart, Germany

Complete contact information is available at:

<https://pubs.acs.org/doi/10.1021/acssensors.9b02314>

### Author Contributions

All authors have given approval to the final version of the manuscript.

## Funding

Baden-Württemberg Stiftung; Bundesministerium für Bildung und Forschung; Deutsche Forschungsgemeinschaft; ERC Advanced Grant COMPLEXPLAS; Ministerium für Wissenschaft, Forschung und Kunst Baden-Württemberg.

## Notes

The authors declare no competing financial interest.

## ■ ACKNOWLEDGMENTS

We gratefully acknowledge financial support by the Deutsche Forschungsgemeinschaft (SPP1839 – Tailored Disorder), by the Bundesministerium für Bildung und Forschung (WasSens 13N8341), by the Baden-Württemberg Stiftung, by ERC Advanced Grant COMPLEXPLAS, and by the Ministerium of Wissenschaft, Forschung und Kunst Baden-Württemberg. We would furthermore like to thank W. Wendlik and A. Geyer from CGS Prozessanalytik GmbH for excellent support and A. Tittl for his valuable contributions to the sensor development.

## ■ REFERENCES

- (1) Edwards, P. P.; Kuznetsov, V. L.; David, W. I. F.; Brandon, N. P. Hydrogen and Fuel Cells: Towards a Sustainable Energy Future. *Energy Policy* **2008**, *36*, 4356–4362.
- (2) Schlapbach, L. Hydrogen-Fuelled Vehicles. *Nature* **2009**, *460*, 809–811.
- (3) Piotrowski, T.; Rozga, P.; Kozak, R. Analysis of Excessive Hydrogen Generation in Transformers in Service. *IEEE Trans. Dielectr. Electr. Insul.* **2015**, *22*, 3600–3607.
- (4) Bodzenta, J.; Burak, B.; Gacek, Z.; Jakubik, W. P.; Kochowski, S.; Urbańczyk, M. Thin Palladium Film as a Sensor of Hydrogen Gas Dissolved in Transformer Oil. *Sens. Actuators, B* **2002**, *87*, 82–87.
- (5) Chen, X.; Huang, L.; Mühlender, H.; Li, G.; Bai, B.; Tan, Q.; Jin, G.; Qiu, C. W.; Zhang, S.; Zentgraf, T. Dual-Polarity Plasmonic Metasurfaces for Visible Light. *Nat. Commun.* **2012**, *3*, 1198.
- (6) Yin, X.; Steinle, T.; Huang, L.; Taubner, T.; Wuttig, M.; Zentgraf, T.; Giessen, H. Beam Switching and Bifocal Zoom Lensing Using Active Plasmonic Metasurfaces. *Light: Sci. Appl.* **2017**, *6*, e17016–e17016.
- (7) Linnenbank, H.; Grynko, Y.; Förstner, J.; Linden, S. Second Harmonic Generation Spectroscopy on Hybrid Plasmonic/Dielectric Nanoantennas. *Light: Sci. Appl.* **2016**, *5*, e16013–e16013.
- (8) Tittl, A.; Michel, A. K. U.; Schäferling, M.; Yin, X.; Gholipour, B.; Cui, L.; Wuttig, M.; Taubner, T.; Neubrech, F.; Giessen, H. A Switchable Mid-Infrared Plasmonic Perfect Absorber with Multispectral Thermal Imaging Capability. *Adv. Mater.* **2015**, *27*, 4597–4603.
- (9) Zhao, R.; Sain, B.; Wei, Q.; Tang, C.; Li, X.; Weiss, T.; Huang, L.; Wang, Y.; Zentgraf, T. Multichannel Vectorial Holographic Display and Encryption. *Light: Sci. Appl.* **2018**, *7*, 95.
- (10) Minovich, A. E.; Peter, M.; Bleckmann, F.; Becker, M.; Linden, S.; Zayats, A. V. Reflective Metasurfaces for Incoherent Light to Bring Computer Graphics Tricks to Optical Systems. *Nano Lett.* **2017**, *17*, 4189–4193.
- (11) Liu, N.; Tang, M. L.; Hentschel, M.; Giessen, H.; Alivisatos, A. P. Nanoantenna-Enhanced Gas Sensing in a Single Tailored Nanofocus. *Nat. Mater.* **2011**, *10*, 631–636.
- (12) Liu, N.; Mesch, M.; Weiss, T.; Hentschel, M.; Giessen, H. Infrared Perfect Absorber and Its Application as Plasmonic Sensor. *Nano Lett.* **2010**, *10*, 2342–2348.
- (13) Bagheri, S.; Strohfeldt, N.; Sterl, F.; Berrier, A.; Tittl, A.; Giessen, H. Large-Area Low-Cost Plasmonic Perfect Absorber Chemical Sensor Fabricated by Laser Interference Lithography. *ACS Sensors* **2016**, *1*, 1148–1154.
- (14) Tittl, A.; Giessen, H.; Liu, N. Plasmonic Gas and Chemical Sensing. *Nanophotonics* **2014**, *3*, 157–180.
- (15) Strohfeldt, N.; Tittl, A.; Giessen, H. Long-Term Stability of Capped and Buffered Palladium-Nickel Thin Films and Nanostruc-

tures for Plasmonic Hydrogen Sensing Applications. *Opt. Mater. Express* **2013**, *3*, 194.

(16) Sterl, F.; Strohfeldt, N.; Walter, R.; Griessen, R.; Tittl, A.; Giessen, H. Magnesium as Novel Material for Active Plasmonics in the Visible Wavelength Range. *Nano Lett.* **2015**, *15*, 7949–7955.

(17) Strohfeldt, N.; Tittl, A.; Schäferling, M.; Neubrech, F.; Kreibig, U.; Griessen, R.; Giessen, H. Yttrium Hydride Nanoantennas for Active Plasmonics. *Nano Lett.* **2014**, *14*, 1140–1147.

(18) Strohfeldt, N.; Zhao, J.; Tittl, A.; Giessen, H. Sensitivity Engineering in Direct Contact Palladium-Gold Nano-Sandwich Hydrogen Sensors. *Opt. Mater. Express* **2015**, *5*, 2525–2535.

(19) Nugroho, F. A. A.; Darmadi, I.; Zhdanov, V. P.; Langhammer, C. Universal Scaling and Design Rules of Hydrogen-Induced Optical Properties in Pd and Pd-Alloy Nanoparticles. *ACS Nano* **2018**, *12*, 9903–9912.

(20) Nugroho, F. A. A.; Darmadi, I.; Cusinato, L.; Susarrey-Arce, A.; Schreuders, H.; Bannenberg, L. J.; da Silva Fanta, A. B.; Kadkhodazadeh, S.; Wagner, J. B.; Antosiewicz, T. J.; et al. Metal–Polymer Hybrid Nanomaterials for Plasmonic Ultrafast Hydrogen Detection. *Nat. Mater.* **2019**, *18*, 489–495.

(21) Walter, R.; Tittl, A.; Berrier, A.; Sterl, F.; Weiss, T.; Giessen, H. Large-Area Low-Cost Tunable Plasmonic Perfect Absorber in the Near Infrared by Colloidal Etching Lithography. *Adv. Opt. Mater.* **2015**, 398–403.

(22) Tittl, A.; Mai, P.; Taubert, R.; Dregely, D.; Liu, N.; Giessen, H. Palladium-Based Perfect Plasmonic Absorber in the Visible and Its Application to Hydrogen Sensing. *Nano Lett.* **2011**, *11*, 4366.

(23) Tittl, A.; Harats, M. G.; Walter, R.; Yin, X.; Schäferling, M.; Liu, N.; Rapaport, R.; Giessen, H. Quantitative Angle-Resolved Small-Spot Reflectance Measurements on Plasmonic Perfect Absorbers: Impedance Matching and Disorder Effects. *ACS Nano* **2014**, *8*, 10885–10892.

(24) Sterl, F.; Strohfeldt, N.; Both, S.; Herkert, E.; Weiss, T.; Giessen, H. Design Principles for Sensitivity Optimization in Plasmonic Hydrogen Sensors. *ACS Sensors* **2020**, DOI: 10.1021/acssensors.9b02436.

(25) Teutsch, T.; Strohfeldt, N.; Sterl, F.; Warsewa, A.; Herkert, E.; Paone, D.; Giessen, H.; Tarin, C. Mathematical Modeling of a Plasmonic Palladium-Based Hydrogen Sensor. *IEEE Sens. J.* **2018**, *18*, 1946–1959.

(26) Griessen, R.; Strohfeldt, N.; Giessen, H. Thermodynamics of the Hybrid Interaction of Hydrogen with Palladium Nanoparticles. *Nat. Mater.* **2016**, *15*, 311–317.

(27) Langhammer, C.; Zorić, I.; Kasemo, B.; Clemens, B. M. Hydrogen Storage in Pd Nanodisks Characterized with a Novel Nanoplasmonic Sensing Scheme. *Nano Lett.* **2007**, *7*, 3122–3127.

(28) Wadell, C.; Syrenova, S.; Langhammer, C. Plasmonic Hydrogen Sensing with Nanostructured Metal Hydrides. *ACS Nano* **2014**, *8*, 11925–11940.

(29) Syrenova, S.; Wadell, C.; Nugroho, F. A. A.; Gschneidner, T. A.; Diaz Fernandez, Y. A.; Nalin, G.; Świtlik, D.; Westerlund, F.; Antosiewicz, T. J.; Zhdanov, V. P.; et al. Hydride Formation Thermodynamics and Hysteresis in Individual Pd Nanocrystals with Different Size and Shape. *Nat. Mater.* **2015**, *14*, 1236–1244.

(30) Narayan, T. C.; Hayee, F.; Baldi, A.; Leen Koh, A.; Sinclair, R.; Dionne, J. A. Direct Visualization of Hydrogen Absorption Dynamics in Individual Palladium Nanoparticles. *Nat. Commun.* **2017**, *8*, 1–8.

(31) Shegai, T.; Langhammer, C. Hydride Formation in Single Palladium and Magnesium Nanoparticles Studied by Nanoplasmonic Dark-Field Scattering Spectroscopy. *Adv. Mater.* **2011**, *23*, 4409–4414.

(32) Baldi, A.; Narayan, T. C.; Koh, A. L.; Dionne, J. A. In Situ Detection of Hydrogen-Induced Phase Transitions in Individual Palladium Nanocrystals. *Nat. Mater.* **2014**, *13*, 1143–1148.

(33) Palm, K. J.; Murray, J. B.; McClure, J. P.; Leite, M. S.; Munday, J. N. In Situ Optical and Stress Characterization of Alloyed Pd<sub>x</sub>Au<sub>1-x</sub>Hydrides. *ACS Appl. Mater. Interfaces* **2019**, *11*, 45057–45067.

(34) Bannenberg, L. J.; Boelsma, C.; Schreuders, H.; Francke, S.; Steinke, N. J.; van Well, A. A.; Dam, B. Optical Hydrogen Sensing

beyond Palladium: Hafnium and Tantalum as Effective Sensing Materials. *Sens. Actuators, B* **2019**, *283*, 538–548.

(35) Bannenberg, L. J.; Nugroho, F. A. A.; Schreuders, H.; Norder, B.; Trinh, T. T.; Steinke, N. J.; Van Well, A. A.; Langhammer, C.; Dam, B. Direct Comparison of PdAu Alloy Thin Films and Nanoparticles upon Hydrogen Exposure. *ACS Appl. Mater. Interfaces* **2019**, *11*, 15489–15497.

(36) Westerwaal, R. J.; Rooijmans, J. S. A.; Leclercq, L.; Gheorghe, D. G.; Radeva, T.; Mooij, L.; Mak, T.; Polak, L.; Slaman, M.; Dam, B.; et al. Nanostructured Pd-Au Based Fiber Optic Sensors for Probing Hydrogen Concentrations in Gas Mixtures. *Int. J. Hydrogen Energy* **2013**, *38*, 4201–4212.

(37) Boelsma, C.; Bannenberg, L. J.; van Setten, M. J.; Steinke, N.-J.; van Well, A. A.; Dam, B. Hafnium - An Optical Hydrogen Sensor Spanning Six Orders in Pressure. *Nat. Commun.* **2017**, *8*, 1–8.

(38) Schröder, V.; Emonts, B.; Janßen, H.; Schulze, H. P. Explosion Limits of Hydrogen/Oxygen Mixtures at Initial Pressures up to 200 Bar. *Chem. Eng. Technol.* **2004**, *27*, 847–851.

(39) Buttner, W. J.; Post, M. B.; Burgess, R.; Rivkin, C. An Overview of Hydrogen Safety Sensors and Requirements. *Int. J. Hydrogen Energy* **2011**, *36*, 2462–2470.

(40) Hübert, T.; Boon-Brett, L.; Palmisano, V.; Bader, M. A. Developments in Gas Sensor Technology for Hydrogen Safety. *Int. J. Hydrogen Energy* **2014**, *39*, 20474–20483.

(41) Fedtke, P.; Wienecke, M.; Bunescu, M.-C.; Pietrzak, M.; Deistung, K.; Borchardt, E. Hydrogen Sensor Based on Optical and Electrical Switching. *Sens. Actuators, B* **2004**, *100*, 151–157.

(42) Albers, P.; Pietsch, J.; Parker, S. F. Poisoning and Deactivation of Palladium Catalysts. *J. Mol. Catal. A: Chem.* **2001**, 275.

(43) Conti, R. S.; Hertzberg, M. Thermal Autoignition Temperatures for Hydrogen-Air and Methane-Air Mixtures. *J. Fire Sci.* **1988**, *6*, 348–355.

(44) Darmadi, I.; Nugroho, F. A. A.; Kadkhodazadeh, S.; Wagner, J. B.; Langhammer, C. Rationally Designed PdAuCu Ternary Alloy Nanoparticles for Intrinsically Deactivation-Resistant Ultrafast Plasmonic Hydrogen Sensing. *ACS Sensors* **2019**, *4*, 1424–1432.

(45) Zhang, Y.-n.; Peng, H.; Qian, X.; Zhang, Y.; An, G.; Zhao, Y. Recent Advancements in Optical Fiber Hydrogen Sensors. *Sens. Actuators, B* **2017**, *244*, 393–416.